Characterization of mechanical and biochemical properties of developing embryonic tendon

Joseph E. Marturano[a], Jeffrey D. Arena[a], Zachary A. Schiller[a], Irene Georgakoudi[a], and Catherine K. Kuo[a,b,1]

[a]Department of Biomedical Engineering, Tufts University, Medford, MA 02155; and [b]Cell, Molecular, and Developmental Biology Program, Sackler School of Graduate Biomedical Sciences, Tufts University School of Medicine, Boston, MA 02111

Tendons have uniquely high tensile strength, critical to their function to transfer force from muscle to bone. When injured, their innate healing response results in aberrant matrix organization and functional properties. Efforts to regenerate tendon are challenged by limited understanding of its normal development. Consequently, there are few known markers to assess tendon formation and parameters to design tissue engineering scaffolds. We profiled mechanical and biological properties of embryonic tendon and demonstrated functional properties of developing tendon are not wholly reflected by protein expression and tissue morphology. Using force volume-atomic force microscopy, we found that nano- and microscale tendon elastic moduli increase nonlinearly and become increasingly spatially heterogeneous during embryonic development. When we analyzed potential biochemical contributors to modulus, we found statistically significant but weak correlation between elastic modulus and collagen content, and no correlation with DNA or glycosaminoglycan content, indicating there are additional contributors to mechanical properties. To investigate collagen cross-linking as a potential contributor, we inhibited lysyl oxidase-mediated collagen cross-linking, which significantly reduced tendon elastic modulus without affecting collagen morphology or DNA, glycosaminoglycan, and collagen content. This suggests that lysyl oxidase-mediated cross-linking plays a significant role in the development of embryonic tendon functional properties and demonstrates that changes in cross-links alter mechanical properties without affecting matrix content and organization. Taken together, these data demonstrate the importance of functional markers to assess tendon development and provide a profile of tenogenic mechanical properties that may be implemented in tissue engineering scaffold design to mechanoregulate new tendon regeneration.

musculoskeletal | second harmonic generation

Tendon is a principal tissue involved in movement, functioning primarily to transfer loads from muscle to bone. Acute and chronic tendon injuries are significant clinical problems due to poor innate healing ability and drawbacks associated with surgical repair (1, 2). In 2006, musculoskeletal symptoms were the second most frequent reason for physician visits in the United States, resulting in over 130 million visits at a cost of nearly $850 billion (3). Almost half of these visits involved tendons and ligaments, with incidence expected to rise with an aging population. Thus, efforts have focused on engineering new tissues for replacement, although this has been challenged by a paucity of markers with which to assess functional tendon development and few known cues to direct differentiation and new tissue formation.

Characterization of tendon formation in embryonic or engineered tissue has typically relied on molecular markers, as well as matrix composition and organization (4–9). Although useful for assessing cell differentiation and ECM deposition during tissue formation, these characterizations may not reflect functional property elaboration. During normal development, cells secrete, organize, and cross-link ECM molecules, presumably imparting mechanical properties to the tissue (10, 11). However, mechanical properties have not been measured, and particular cross-linking mechanisms during tendon formation are not known.

An available profile of tendon mechanical properties over the full range of embryonic development would provide functional markers for characterization of proper tissue assembly.

Embryonic tendon is highly cellular and begins with a sparse, disorganized collagen fiber matrix. In contrast, mature, functional tendon is composed primarily of highly aligned, cross-linked collagen fibers that are integral to its uniquely high tensile strength and function. Reported primary contributors to adult tendon mechanical properties include collagen content (12), fiber alignment (13), fibril length and diameter (8), and cross-linking (14). Enzymatic [lysyl oxidase (LOX)-mediated] cross-links and glycosaminoglycans (GAGs) have been implicated in the bridging of adjacent collagen molecules, and therefore may play a significant role in tendon mechanical properties (15, 16). Although the influence of these cross-links on mechanical properties of adult and aging tendon has been investigated, findings are inconsistent and very little is known about their contributions to developing embryonic tendon. Understanding how mechanical properties elaborate during tendon development may lead to tissue engineering strategies that integrate cues to target mechanisms of matrix assembly during functional tissue formation.

Uniaxial tensile testing is most commonly used to characterize the bulk mechanical properties of adult tendon, which are important indicators of tissue function. Unfortunately, the small size and fragility of embryonic tendon limit the use of tensile testing to the latest stages of development (8, 17). Alternatively, atomic force microscopy (AFM) can measure indentation modulus of small and fragile materials, and can detect local variations at micro- and nanoscales. AFM has been used to characterize various tissues mechanically, including growth plate cartilage (18), articular cartilage (19–21), and embryonic cardiac tissue (22). Force volume (FV)-AFM, in particular, captures tissue height measurements and force values simultaneously, generating maps of tissue topography and corresponding mechanical properties, as well as providing information about regional variations in tissue structure and modulus. Additionally, in contrast to bulk testing that describes the whole tissue as a composite material, nano- and microscale indentation testing reflects material properties at the local (e.g., cellular) level that may be particularly relevant as mechanical cues experienced by cells during tissue development.

Characterizing nano- and microscale structure and mechanical properties during embryonic tendon development may identify physical cues that direct differentiation toward the tendon lineage (tenogenesis), because the properties of the ECM greatly

influence the mechanical microenvironment of the cell. Substrate stiffness has been shown to direct stem cell differentiation toward various nontendon phenotypes (23), and hydrogels with time-dependent material properties have enhanced cardiomyocyte differentiation (24, 25). Theoretical predictions suggest mechanical forces contribute to tendon development during knee morphogenesis, although the focus was on load transfer rather than tissue properties (20). We demonstrated cyclical loading modulates tenogenesis of mesenchymal stem cells (26); however, due to a lack of information about the mechanical properties of developing tendon, we did not investigate the effects of substrate modulus. Taken together, the effects of substrate stiffness have not been studied but, similar to loading, may influence tenogenesis. Characterizing embryonic tendon mechanical properties would provide parameters with which to design scaffolds to investigate mechanoregulation of tenogenic differentiation and tissue formation.

Our objective was to characterize the nano- and microscale modulus of embryonic tendon during development and to elucidate potential mechanisms of mechanical property elaboration. We hypothesized that functional properties would increase during development and their elaboration would be a function of collagen cross-link formation. We used FV-AFM to characterize indentation modulus and temporally correlated changes in modulus with quantitative changes in biochemical composition and tissue structure. We also used multiphoton microscopy to correlate variations in elastic modulus spatially with biochemical composition. Finally, we examined enzymatic collagen cross-linking contribution to developing tendon mechanical properties by inhibiting LOX activity. With this study, we aimed to develop a profile of functional properties that describe normal tendon formation and to understand how ECM composition relates to these functional markers.

Results

Elastic Modulus and Topography of Embryonic Tendon.
Chick calcaneus tendons between Hamburger and Hamilton (27) stage (HH) 28 and HH 43 were dissected, cryosectioned, and indentation-tested in PBS (without Ca^{2+} or Mg^{2+}) using FV-AFM (Fig. 1A). Force-displacement curves showed clear mechanical differences between stages, and regions of tip-sample contact with nonzero slope were predominantly linear (Fig. 1B).

Elastic moduli were calculated from either standard curves based on agarose gel measurements (Fig. S1) or Hertzian theory equations (28). Nano- and microscale moduli exhibited a small increase between HH 28 and 30 ($P = 0.11$ for nanoscale, $P = 0.66$ for microscale); changed minimally between HH 30 and 38; and then increased significantly from HH 38–43, where modulus at each stage was significantly different from the preceding stage ($P < 0.05$) (Fig. 1C). On average, microscale modulus was 3.2-fold larger than nanoscale modulus when analyzed with the gel standard (5–108 kPa and 7–21 kPa, respectively; $P < 0.05$) and twofold larger when analyzed with the Hertz model (9–31 kPa and 5–17 kPa, respectively; $P < 0.05$) (Fig. 1C). The coefficient of variation of elastic modulus increased with development, particularly at later stages (HH 41–43) (Fig. 1C). Similarly, there was greater heterogeneity in maps of modulus and tissue topography at later stages (Fig. 1D). To confirm the variability in spatial correlation between topography and modulus maps (Fig. 1D), we confirmed FV-AFM topography with contact mode AFM (Fig. S2).

Qualitative Characterization of Biochemical Composition and Structure of Developing Tendon.
With second harmonic generation (SHG) imaging and trichrome staining, collagen fibers were first detected at HH 35, subsequently increasing in density and organization through HH 41–43 (Fig. 2 A and B). Although Pic-
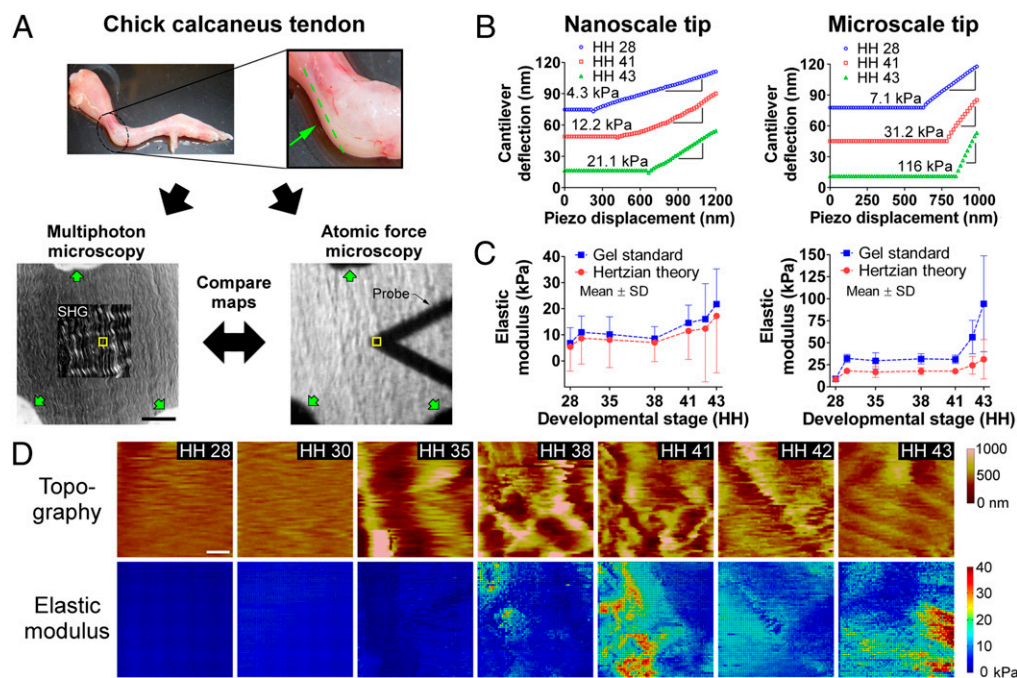

Fig. 1. FV-AFM results. (A, Upper) HH 43 limb with calcaneus tendon highlighted; the sectioning plane is shown in green. (Lower) Cryosection of tendon visualized with multiphoton microscopy (SHG; Left) and brightfield microscopy with the AFM probe in view (Right). Yellow boxes show the AFM-probed area. Verhoeff stain (green arrows) was used to mark the same regions for multiphoton microscopy and FV-AFM measurements. (Scale bar, 50 μm.) (B) Force-displacement AFM curves of tendon from HH 28–43. Slopes of linear regions were used to calculate modulus. (C) Tendon elastic modulus measured via FV-AFM as a function of developmental stage, calculated with agarose gel standards and Hertzian theory. Modulus increased nonlinearly during development, with the greatest increases between HH 28 and 30 and after HH 38 (n = 5). (D) FV-AFM topography and nanoscale elastic modulus maps of embryonic tendon from HH 28–43. Both showed increasing heterogeneity during development. (Scale bar, 2 μm.)
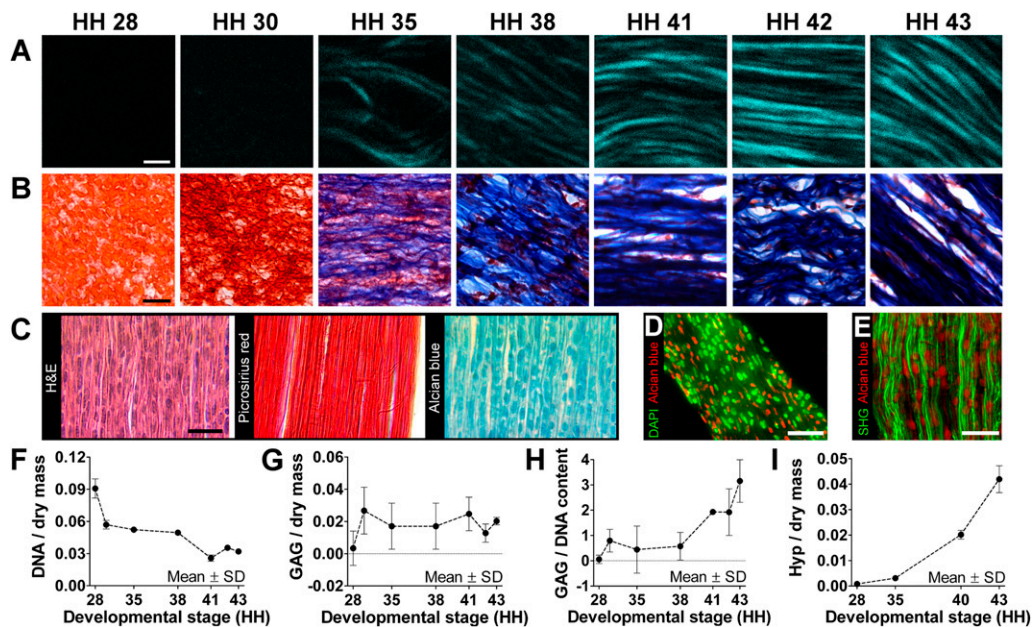
Fig. 2. Morphological and biochemical characterization. (*A*) SHG imaging showed increases in collagen density and organization during tendon development. (Scale bar, 2 μm.) (*B*) Trichrome staining showed a decrease in cellularity (red) and increase in collagen content (blue) with development. (Scale bar, 20 μm.) (*C*) HH 43 tendon sections show high density of cell nuclei (H&E), aligned collagen (Picrosirius red), and GAG deposits (Alcian blue). (Scale bar, 25 μm.) (*D*) Cell nuclei (green) and GAG deposits (red) were similar in shape and size but spatially distinct in HH 43 tendon. (Scale bar, 25 μm.) (*E*) GAG deposits (red) appeared closely associated with collagen fibers (green). (Scale bar, 20 μm.) From HH 28–43, DNA-to-dry mass content decreased by 67% (*F*; n = 3); GAG-to-dry mass content remained relatively constant (*G*; n = 3); and GAG-to-DNA ratio (*H*; n = 3) and Hyp-to-dry mass ratio (*I*; n = 3), representative of collagen content, increased dramatically.

rosirius red staining highlighted densely aligned collagen fibers by HH 43, the tissue was still highly cellular, as shown with H&E staining (Fig. 2*C*). Interestingly, Alcian blue staining showed a high density of GAG deposits, similar in size and shape to cell nuclei (Fig. 2*C*). These GAG deposits appeared spatially distinct from cell nuclei (Fig. 2*D* and Fig. S3*A*) and closely associated with collagen fibers (Fig. 2*E*).

Quantitative Characterization of Biochemical Composition of Developing Tendon. DNA-to-dry mass ratio progressively decreased by 67% (Fig. 2*F*), whereas total GAG-to-dry mass ratio remained relatively constant with time (Fig. 2*G*). Total GAG-to-DNA ratio remained less than 1 until HH 38, after which it increased up to a ratio of 3 (Fig. 2*H*). Hydroxyproline (Hyp) content, representative of collagen content, increased nearly exponentially during development as a function of dry mass (Fig. 2*I*) and DNA content (Fig. S3*B*).

Spatial Correlation of Elastic Moduli, Biochemical Composition, and Structure of Embryonic Tendon. To examine spatial relationships between mechanical properties and collagen fibers, GAGs, and cell nuclei, we correlated elastic modulus maps with multiphoton microscopy images of the same tissue regions in HH 43 tendon. Qualitatively, nanoscale elastic modulus appeared to be positively correlated with collagen fibers (high modulus in regions with fibers) and negatively correlated with cell nuclei (low modulus in regions of nuclei), and it showed little correlation with GAG deposits (Fig. 3*A*, control). Reflective of these findings, Pearson's correlation coefficient (*r*) between modulus and collagen fibers was weak but significant (*r* = 0.13, *P* < 0.05) compared with no correlation between modulus and cell nuclei (*r* = −0.07, *P* = 0.23) or total GAGs (*r* = −0.04, *P* = 0.50) (Fig. 3*B*, control).

Contribution of LOX-Mediated Cross-Linking to Mechanical Property Elaboration. To investigate collagen cross-linking as a potential mechanism of mechanical property elaboration, we treated chicks

in ovo with β-aminopropionitrile (BAPN). BAPN binds the active site of LOX to inhibit the enzyme in collagen and elastin cross-linking (29). Elastin was not detected in embryonic tendon (Fig. S4); thus, we focused on collagen. BAPN treatment for 24 h *in ovo* did not appear to affect collagen fiber density or organization (*P* ≥ 0.16; Fig. 4*A* and Fig. S5). These observations were corroborated by biochemical analyses, which demonstrated no significant differences in Hyp content from HH 28–43 between saline and BAPN doses (*P* ≥ 0.51; Fig. 4*B*) or in cellularity, dry mass, or GAG content of HH 43 tendons (*P* ≥ 0.41; Fig. S6 *A* and *B*).

Despite no detected biochemical changes, BAPN treatment reduced elastic modulus by up to 38.8% at HH 40 (*P* < 0.05) and 68.4% at HH 43 (*P* < 0.001) (Fig. 4*C*). Histograms at HH 40 and 43 indicated that BAPN restricted modulus to a maximum of 15 kPa, compared with 40 kPa with saline (Fig. S6*C*). Also, there was no longer a significant difference in Pearson's correlation coefficient between modulus and collagen fibers, compared with modulus and cell nuclei or GAGs (*P* = 0.59; Fig. 3*B*).

To investigate if BAPN adversely affected cell function *in ovo*, we treated HH 42 embryonic tendon cells in vitro with BAPN at concentrations reported to inhibit LOX activity in vitro (29). There were no significant differences in cell viability, proliferation, or metabolic activity after 72 h (*P* ≥ 0.40; Fig. S7). In addition, to assess potential systemic effects of *in ovo* BAPN treatment on the developing tendon, we treated HH 40 explant cultures with BAPN for 24 h and measured modulus with FV-AFM. Modulus of tendon explants decreased by 45% with BAPN treatment (Fig. S8*A*), similar to *in ovo* reductions (Fig. 4*C*).

Discussion

In this study, we characterized chick tendon mechanical property elaboration throughout the full range of embryonic tendon development. One goal of our study was to characterize functional markers of tendon development. To date, assessments of em-
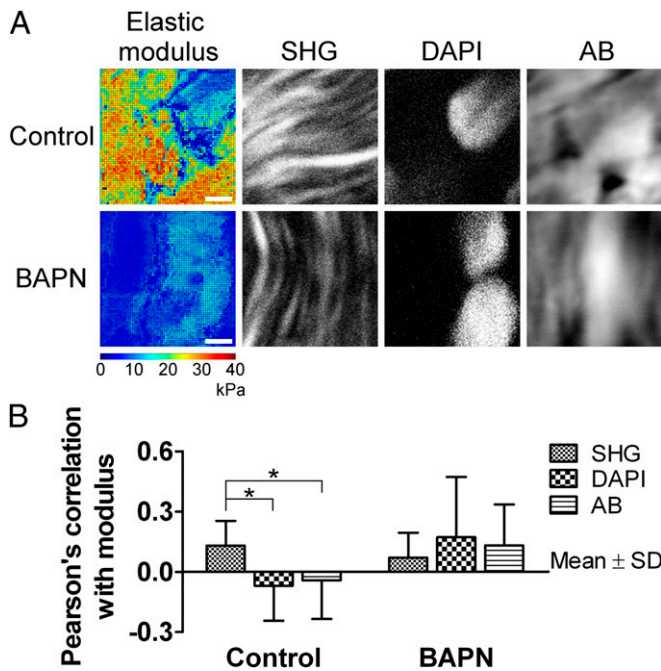
Fig. 3. Spatial correlation of nanoscale modulus with collagen fibers (SHG), cell nuclei (DAPI), and GAGs (Alcian blue). Collagen fibers seemed more spatially correlated to elastic modulus than cell nuclei or GAGs when normally cross-linked. (*A*) Comparison of modulus maps (color images) with microscopy (black and white images) of the same areas. In control tissue, there appeared to be correlation between high-modulus regions and collagen fibers, and between low-modulus regions and cell nuclei and GAGs. After BAPN treatment, average modulus was reduced and areas of GAGs and cell nuclei appeared to be more correlated with modulus. (Scale bars, 2 µm.) (*B*) Pearson's correlation coefficient between FV-AFM modulus maps and multiphoton microscopy ($n = 10$). In control samples, collagen fibers were weakly but significantly more correlated than cell nuclei or GAGs (*$P < 0.05$). This effect was lost with BAPN treatment ($P = 0.59$).

bryonic tendon development and in vitro tenogenesis have focused primarily on molecular regulators of differentiation and matrix protein composition and organization (5–7, 9) rather than functional properties. In contrast, we characterized mechanical properties and their potential contributors as markers to assess functional embryonic tendon formation. Notably, we demonstrate that embryonic tendon functional properties cannot be predicted solely by quantitative changes in ECM composition and morphology. When enzymatic cross-linking of collagen was inhibited, mechanical properties were significantly reduced, despite no detectable changes in cellularity, GAG, or collagen

content or organization. This was a significant and unique finding, demonstrating that functional property elaboration during proper tendon tissue formation throughout development and tissue engineering cannot be adequately assessed by gene and protein expression or matrix structure.

Another goal of our study was to characterize tendon mechanical properties to derive physical cues to inform tendon regeneration strategies, because embryonic mechanical properties at the cell-length scale may be used as mechanoregulatory cues to guide new tendon formation. Physical cues, such as substrate stiffness, are known to direct stem cell lineage commitment and self-renewal (23, 30). Recently, scaffolds that stiffen over time have been developed to mimic the mechanical property changes of tissues during development, wound healing, and disease (24, 31). These dynamic scaffolds enhanced differentiation toward myocardial (24), adipogenic, and osteogenic lineages (31) over scaffolds with static mechanical properties. Here, we characterized multiple facets of the developing tendon (e.g., topography, matrix content and organization, mechanical properties) as scaffold design parameters that may direct tenogenesis and neotendon formation.

Previous studies of embryonic tendon mechanical properties have focused primarily on bulk tensile testing at late embryonic and early postnatal stages (8, 32). However, even at the latest embryonic stages, bulk tensile elastic modulus values of chick tendon differed by nearly 100-fold between studies [210 kPa (8) vs. 20 MPa (33) at day 14], perhaps due to challenges with handling small and delicate tissues. In contrast, we used micro- and nanoscale indentation testing over the full range of embryonic tendon development. In our study, both nano- and microscale indentation moduli increased during development, with dramatic increases after HH 38. The late-stage modulus increases correlated well with reported trends for collagen fibril length and bulk tensile modulus in embryonic tendon. Collagen fibril length has been reported to increase nearly fivefold via lateral associations between ends of adjacent fibril segments in embryonic chick tendons from HH 38–42 (7), presumably leading to a near doubling in bulk tensile modulus during HH 40–43 (8).

We found microscale moduli were larger than nanoscale moduli, in agreement with cartilage studies. In adult porcine articular cartilage, microscale moduli were 100-fold greater than nanoscale moduli and two- to 10-fold lower than millimeter-scale measurements (21). Another study used a gel-nanofiber model to demonstrate that a nanoscale tip probes single collagen fibrils and proteoglycan components of cartilage, whereas a microscale tip measures a cross-linked network (28). Accordingly, nanoscale moduli were, on average, two-to threefold lower than microscale moduli in our study, and both were one to three orders of magnitude below reported chick tendon bulk tensile moduli (8, 33). We also measured an increase in the SD of average
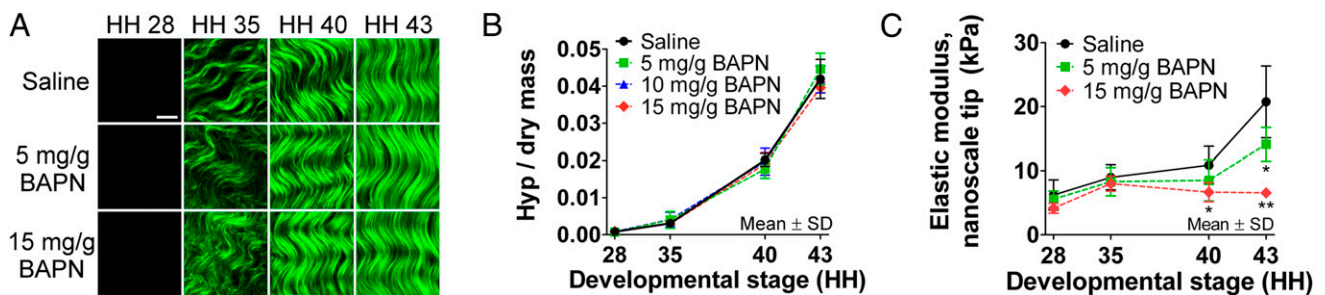
Fig. 4. Effects of BAPN treatment to inhibit LOX activity. (*A*) SHG images showed no apparent differences in collagen microstructure with BAPN treatment compared with a saline control. (Scale bar, 10 µm.) (*B*) BAPN treatment also had no effect on Hyp content, representative of collagen content, during development ($P \geq 0.51$; $n = 3$). (*C*) BAPN treatment significantly reduced tendon elastic modulus measured with a nanoscale tip by 38% at HH 40 (*$P < 0.05$) and by 68% at HH 43 (**$P < 0.001$; $n = 5$).

modulus as a function of developmental stage, with the greatest variability from HH 41–43. Perhaps, at early stages (e.g., HH 28), the AFM probe measured primarily cells and relatively little disorganized matrix, whereas at later stages (e.g., HH 43), the probe sensed both cells and an increasingly organized matrix network (Fig. 2 A and B), resulting in more heterogeneous profiles of both mechanical properties and tissue topography. These temporal changes in nano- and microscale elastic modulus, relevant at the cell-length scale, could be mechanoregulating tendon progenitor cell differentiation and function during development.

Studies suggest that proteoglycans contribute to collagen cross-linking and tendon mechanical properties (15, 16). We observed an increase in collagen fiber content and organization during development (Fig. 2 A and B) and found GAG deposits to be closely associated with collagen fibers by HH 43 (Fig. 2E). GAG-to-DNA (Fig. 2H) and Hyp-to-DNA (Fig. S3B) content both increased as a function of stage, suggesting that both GAGs and collagens are actively being synthesized. A nearly 30-fold increase in the Hyp-to-dry mass ratio (Fig. 2I) corroborated qualitative collagen content increases during tendon development (Fig. 2 A and B). GAG-to-dry mass ratio plateaued at HH 30 (Fig. 2G), suggesting total GAGs were being produced at a rate that maintained GAG density as tissue mass increases (Fig. S8B). Reports of dynamic changes in spatiotemporal distribution of various proteoglycans throughout tendon development suggest roles for GAGs in collagen fibrillogenesis and cross-linking (5, 7, 9), although enzymatic digestion of GAGs did not affect bulk elastic modulus in adult murine tendon (34, 35) or microscale modulus in adult bovine cartilage (21). We measured total GAG content in our study; thus, it was not possible to discern trends for specific GAG-containing molecules. Future experiments are needed to delineate specific roles of different GAG-containing molecules that may contribute to developing tendon.

Spatial correlations between topography and elastic modulus were observed in some samples (Fig. 1D) but not in others. Elastic modulus was more spatially correlated with collagen fibers than cells or GAGs, but the correlation coefficient was weak ($r = 0.13$, $P < 0.05$). It was apparent that both topography and modulus became increasingly heterogeneous with development. We chose FV-AFM for its unique utility to assess both regional mechanical properties and topography. Notably, FV-AFM topographical characterization is influenced by sample stiffness, which could be significant for mechanically heterogeneous samples, such as a developing matrix network. However, we found topography maps generated with both contact mode and FV-AFM were comparable, and thus considered that the weak correlations between topography and modulus maps may indicate additional contributors to functional properties, such as cross-linking.

Cross-linking of tendon during embryonic development has been studied very little. In contrast, cross-linking of tendon during maturation and aging has been studied to understand change in function during the adult lifespan. Studies suggest bridging via GAGs and enzymatic and nonenzymatic cross-linking of collagen molecules contribute to mechanical property changes during tendon tissue maturation and aging (14, 36). GAGs have been reported to play a role in regulating collagen cross-linking and fiber diameter during tendon development but were weakly correlated with modulus in our study, and their enzymatic removal was reported to have little effect on mechanical properties, collagen content, or fiber density (7, 15, 34, 35, 37). Nonenzymatic glycation cross-links, such as pentosidine, have shown little mechanical contribution based on studies with rat tail tendons (38).

LOX deaminates lysine and hydroxylysine residues in adjacent collagen molecules to form aldehyde groups that effectively cross-link aligned collagen molecules, thereby enhancing tissue mechanical properties by preventing intermolecular slip (39).

LOX-derived cross-linking increases during adult tendon aging and wound healing (14, 40), and it is believed to contribute significantly to mature tendon mechanical properties, although reports are inconsistent. LOX-derived hydroxylysyl pyridinoline (HP) cross-linking density was significantly correlated to elastic modulus in goat patellar tendon (41) but not in equine superficial digital flexor tendon (42) or human patellar tendon (43). In contrast, there are limited data of collagen cross-linking in embryonic tendon, and the focus was on a single embryonic time point without examining mechanical contributions (44).

In embryonic chick skin and bone, inhibition of LOX activity via BAPN treatment produced profound reductions in mechanical properties (36). Here, we found large reductions in embryonic tendon nanoscale modulus in response to BAPN treatment *in ovo* (Fig. 4C) and in explant culture (Fig. S8A). Despite this, inhibition of LOX activity with BAPN treatment had minimal effects on bulk collagen content, fiber morphology and density (Fig. 4); dry-to-wet mass ratio; GAG content or cellularity *in ovo* (Fig. S6 A and B); or cell proliferation, metabolic activity, or viability in vitro (Fig. S7). In addition, after HH 43 embryonic tendon was treated with BAPN, modulus was no longer significantly spatially correlated with tissue components ($P = 0.59$; Fig. 3B). Taken together, these data suggest that mechanical property elaboration during embryonic tendon development is due, in part, to LOX-mediated collagen cross-linking.

Understanding functional changes during normal development of embryonic tendon may provide a platform with which to study abnormal changes that occur during tendon repair, which results in scar tissue with aberrant matrix composition, morphology, and mechanical properties, despite surgical intervention. These shifts may, in part, be related to cross-linking, because studies have presented evidence that the HP-to-collagen ratio of degenerated human supraspinatus tendons is significantly different from that of age-matched healthy tendons (45). Being able to pinpoint when and how the tendon-healing process deviates from normal tendon formation may enable strategies to intercept and redirect the scarred healing response toward a regenerative response.

Finally, our results provide a profile of functional markers that characterize normal tissue formation. Notably, we demonstrate that cross-linking modifies mechanical resilience in the face of steady collagen content. The findings of this study may enable developmentally inspired tendon engineering strategies. Our study demonstrates that functional properties are an essential complement to gene, protein, and morphological assessments, because the latter are typical metrics of tissue engineering progress that do not fully reflect the proper development of a tissue. This may be significant for normal tissue development and engineered tissue formation, as well as for tissue healing. Because others have shown that musculoskeletal developmental mechanisms in chick commonly parallel those of mouse (6), this study may serve as proof-of-concept for mammalian species. Future studies to characterize cross-linking during development may provide additional insights into mechanical property elaboration during tendon formation, healing, and regeneration.

Materials and Methods

Detailed descriptions of materials and methods used in this study are provided in *SI Materials and Methods*.

***In Ovo*, In Vitro, and Explant Cultures.** All animal procedures received prior approval from the Tufts University Institutional Animal Care and Use Committee board. Chicken embryos were injected *in ovo* with saline or BAPN, incubated for 24 h, and killed between HH 28 and 43. Calcaneal tendons were dissected for FV-AFM or biochemical analysis.

FV-AFM. FV-AFM was used to capture indentation force curves in a 2D array on 20-μm-thick tendon cryosections in Dulbecco's modified PBS (without Ca^{2+}/Mg^{2+}) with either nanoscale (~20 nm) or microscale (5 μm) tips (Fig. S9). Tendons from one leg each of five chicks were measured. Elastic moduli were

derived either empirically (agarose gel standards; Fig. S1) or from Hertzian theory (28).

Biochemical Analysis. Standard absorbance-based protocols were used to determine DNA-, GAG-, and Hyp-to-dry mass ratios with at least three pools of tendons from at least three chicks each (Fig. S9).

Histology. Formalin-fixed tendon tissue was paraffin-embedded, and consecutive 8-μm-thick sections were stained with standard protocols for at least three chicks (both legs each).

Multiphoton Microscopy. Forward SHG from fresh, unfixed tendons was captured on a laser scanning, two-photon microscope with 800 nm of incident light and a 63× (1.2 N.A.) water immersion objective with at least four chicks (both legs each).

Spatial Correlation of FV-AFM with Multiphoton Microscopy. HH 43 chicks ($n = 10$) were treated with either saline or a 15-mg/g BAPN dose for 24 h before tendon harvest (one leg per chick) and cryosectioning (20 μm).

Sections were marked with Verhoeff stain to enable location of the same region for both FV-AFM and multiphoton maps (Fig. 1A). FV-AFM maps were captured; the tissue was fixed in formalin and stained with DAPI and Alcian blue; and images of the surface were captured with multi-photon microscopy for collagen fibers (SHG), cell nuclei (DAPI), and GAGs (Alcian blue).

Statistics. A one-way ANOVA was used with a Dunnett's or Tukey's posttest depending on whether the comparison was against a control group or not, respectively. Data were reported as mean ± SD.

1. Butler DL, Awad HA (1999) Perspectives on cell and collagen composites for tendon repair. *Clin Orthop Relat Res* (367, Suppl):(Suppl):S324–S332.
2. Woo SL, Abramowitch SD, Kilger R, Liang R (2006) Biomechanics of knee ligaments: Injury, healing, and repair. *J Biomech* 39(1):1–20.
3. AAOS (2008) *United States Bone and Joint Decade: The Burden of Musculoskeletal Diseases in the United States* (American Academy of Orthopaedic Surgeons, Rosemont, IL).
4. Kardon G (1998) Muscle and tendon morphogenesis in the avian hind limb. *Development* 125(20):4019–4032.
5. Kuo CK, Petersen BC, Tuan RS (2008) Spatiotemporal protein distribution of TGF-betas, their receptors, and extracellular matrix molecules during embryonic tendon development. *Dev Dyn* 237(5):1477–1489.
6. Schweitzer R, et al. (2001) Analysis of the tendon cell fate using Scleraxis, a specific marker for tendons and ligaments. *Development* 128(19):3855–3866.
7. Birk DE, Nurminskaya MV, Zycband EI (1995) Collagen fibrillogenesis in situ: Fibril segments undergo post-depositional modifications resulting in linear and lateral growth during matrix development. *Dev Dyn* 202(3):229–243.
8. McBride DJ, Trelstad RL, Silver FH (1988) Structural and mechanical assessment of developing chick tendon. *Int J Biol Macromol* 10(4):194–200.
9. Ros MA, Rivero FB, Hinchliffe JR, Hurle JM (1995) Immunohistological and ultrastructural study of the developing tendons of the avian foot. *Anat Embryol (Berl)* 192(6):483–496.
10. Banos CC, Thomas AH, Kuo CK (2008) Collagen fibrillogenesis in tendon development: Current models and regulation of fibril assembly. *Birth Defects Res C Embryo Today* 84(3):228–244.
11. Kjaer M (2004) Role of extracellular matrix in adaptation of tendon and skeletal muscle to mechanical loading. *Physiol Rev* 84(2):649–698.
12. Woo SL, et al. (1980) The biomechanical and biochemical properties of swine tendons—Long term effects of exercise on the digital extensors. *Connect Tissue Res* 7(3):177–183.
13. Lake SP, Miller KS, Elliott DM, Soslowsky LJ (2010) Tensile properties and fiber alignment of human supraspinatus tendon in the transverse direction demonstrate inhomogeneity, nonlinearity, and regional isotropy. *J Biomech* 43(4):727–732.
14. Couppé C, et al. (2009) Mechanical properties and collagen cross-linking of the patellar tendon in old and young men. *J Appl Physiol* 107(3):880–886.
15. Danielsen CC (1982) Mechanical properties of reconstituted collagen fibrils. Influence of a glycosaminoglycan: Dermatan sulfate. *Connect Tissue Res* 9(4):219–225.
16. Robinson PS, et al. (2005) Influence of decorin and biglycan on mechanical properties of multiple tendons in knockout mice. *J Biomech Eng* 127(1):181–185.
17. Beredjiklian PK, et al. (2003) Regenerative versus reparative healing in tendon: A study of biomechanical and histological properties in fetal sheep. *Ann Biomed Eng* 31(10):1143–1152.
18. Allen DM, Mao JJ (2004) Heterogeneous nanostructural and nanoelastic properties of pericellular and interterritorial matrices of chondrocytes by atomic force microscopy. *J Struct Biol* 145(3):196–204.
19. Darling EM, Wilusz RE, Bolognesi MP, Zauscher S, Guilak F (2010) Spatial mapping of the biomechanical properties of the pericellular matrix of articular cartilage measured in situ via atomic force microscopy. *Biophys J* 98(12):2848–2856.
20. Roddy KA, Kelly GM, van Es MH, Murphy P, Prendergast PJ (2011) Dynamic patterns of mechanical stimulation co-localise with growth and cell proliferation during morphogenesis in the avian embryonic knee joint. *J Biomech* 44(1):143–149.
21. Stolz M, et al. (2004) Dynamic elastic modulus of porcine articular cartilage determined at two different levels of tissue organization by indentation-type atomic force microscopy. *Biophys J* 86(5):3269–3283.
22. Jacot JG, Martin JC, Hunt DL (2010) Mechanobiology of cardiomyocyte development. *J Biomech* 43(1):93–98.
23. Engler AJ, Sen S, Sweeney HL, Discher DE (2006) Matrix elasticity directs stem cell lineage specification. *Cell* 126(4):677–689.
24. Young JL, Engler AJ (2011) Hydrogels with time-dependent material properties enhance cardiomyocyte differentiation in vitro. *Biomaterials* 32(4):1002–1009.
25. Kloxin AM, Benton JA, Anseth KS (2010) In situ elasticity modulation with dynamic substrates to direct cell phenotype. *Biomaterials* 31(1):1–8.
26. Kuo CK, Tuan RS (2008) Mechanoactive tenogenic differentiation of human mesenchymal stem cells. *Tissue Eng Part A* 14(10):1615–1627.
27. Hamburger V, Hamilton HL (1951) A series of normal stages in the development of the chick embryo. *J Morphol* 88(1):49–92.
28. Loparic M, et al. (2010) Micro- and nanomechanical analysis of articular cartilage by indentation-type atomic force microscopy: Validation with a gel-microfiber composite. *Biophys J* 98(11):2731–2740.
29. Tang SS, Trackman PC, Kagan HM (1983) Reaction of aortic lysyl oxidase with beta-aminopropionitrile. *J Biol Chem* 258(7):4331–4338.
30. Gilbert PM, et al. (2010) Substrate elasticity regulates skeletal muscle stem cell self-renewal in culture. *Science* 329(5995):1078–1081.
31. Guvendiren M, Burdick JA (2012) Stiffening hydrogels to probe short- and long-term cellular responses to dynamic mechanics. *Nat Commun* 3:792.
32. Ansorge HL, Adams S, Birk DE, Soslowsky LJ (2011) Mechanical, compositional, and structural properties of the post-natal mouse Achilles tendon. *Ann Biomed Eng* 39(7):1904–1913.
33. Kalson NS, et al. (2011) Slow stretching that mimics embryonic growth rate stimulates structural and mechanical development of tendon-like tissue in vitro. *Dev Dyn* 240(11):2520–2528.
34. Rigozzi S, Müller R, Snedeker JG (2009) Local strain measurement reveals a varied regional dependence of tensile tendon mechanics on glycosaminoglycan content. *J Biomech* 42(10):1547–1552.
35. Screen HR, et al. (2005) The influence of noncollagenous matrix components on the micromechanical environment of tendon fascicles. *Ann Biomed Eng* 33(8):1090–1099.
36. Fry P, Harkness ML, Harkness RD, Nightingale M (1962) Mechanical properties of tissues of lathyritic animals. *J Physiol* 164:77–89.
37. Svensson RB, Hassenkam T, Hansen P, Kjaer M, Magnusson SP (2011) Tensile force transmission in human patellar tendon fascicles is not mediated by glycosaminoglycans. *Connect Tissue Res* 52(5):415–421.
38. Andreassen TT, Oxlund H, Danielsen CC (1988) The influence of non-enzymatic glycosylation and formation of fluorescent reaction products on the mechanical properties of rat tail tendons. *Connect Tissue Res* 17(1):1–9.
39. Barenberg SA, Filisko FE, Geil PH (1978) Ultrastructural deformation of collagen. *Connect Tissue Res* 6(1):25–35.
40. Moriguchi T, Fujimoto D (1978) Age-related changes in the content of the collagen crosslink, pyridinoline. *J Biochem* 84(4):933–935.
41. Ng GY, Oakes BW, Deacon OW, McLean ID, Eyre DR (1996) Long-term study of the biochemistry and biomechanics of anterior cruciate ligament-patellar tendon autografts in goats. *J Orthop Res* 14(6):851–856.
42. Thorpe CT, Stark RJ, Goodship AE, Birch HL (2010) Mechanical properties of the equine superficial digital flexor tendon relate to specific collagen cross-link levels. *Equine Vet J Suppl* 42(38):538–543.
43. Hansen P, et al. (2010) Lower strength of the human posterior patellar tendon seems unrelated to mature collagen cross-linking and fibril morphology. *J Appl Physiol* 108(1):47–52.
44. Snowden JM, Eyre DR, Swann DA (1982) Vitreous structure. VI. Age-related changes in the thermal stability and crosslinks of vitreous, articular cartilage and tendon collagens. *Biochim Biophys Acta* 706(2):153–157.
45. Bank RA, TeKoppele JM, Oostingh G, Hazleman BL, Riley GP (1999) Lysylhydroxylation and non-reducible crosslinking of human supraspinatus tendon collagen: changes with age and in chronic rotator cuff tendinitis. *Ann Rheum Dis* 58(1):35–41.

BIOPHYSICS AND
COMPUTATIONAL BIOLOGY

ENGINEERING